

# ABSORPTION OF 10–200 GeV GAMMA RAYS BY RADIATION FROM BLR IN BLAZARS

H. T. Liu<sup>1,2</sup> and J. M. Bai<sup>1</sup>

liuhongtao1111@hotmail.com and baijinming@ynao.ac.cn

## ABSTRACT

In this paper, we study the photon-photon pair production optical depth for gamma-rays with energies from 10 to 200 GeV emitted by powerful blazars due to the diffuse radiation field of broad line region (BLR). There are four key parameters in the BLR model employed to determine the  $\gamma$ – $\gamma$  attenuation optical depth of these gamma-rays. They are the gamma-ray emitting radius  $R_\gamma$ , the BLR luminosity  $L_{\text{BLR}}$ , the BLR half thickness  $h$  and the ratio  $\tau_{\text{BLR}}/f_{\text{cov}}$  of the Thomson optical depth to the covering factor of BLR. For FSRQs, on average, it is impossible for gamma-rays with energies from 10 to 200 GeV to escape from the diffuse radiation field of the BLR. If *GLAST* could detect these gamma-rays for most of FSRQs, the gamma-ray emitting region is likely to be outside the cavity formed by the BLR. Otherwise, the emitting region is likely to be inside the BLR cavity. As examples, we estimate the photon-photon absorption optical depth of gamma-rays with energies from 10 to 200 GeV for two powerful blazars, HFSRQ PKS 0405–123 and FSRQ 3C 279. Comparing our results with *GLAST* observations in the future could test whether the model employed and the relevant assumptions in this paper are reliable and reasonable, and then limit constraints on the position of the gamma-ray emitting region relative to the BLR and the properties of the BLR.

*Subject headings:* galaxies: active — galaxies: jets — gamma rays: theory — quasars: individual (3C 279, PKS 0405–123)

---

<sup>1</sup>National Astronomical Observatories/Yunnan Astronomical Observatory, the Chinese Academy of Sciences, Kunming, Yunnan 650011, P. R. China.

<sup>2</sup>Graduate School of the Chinese Academy of Sciences, Beijing, P. R. China; send offprint requests to liuhongtao1111@hotmail.com

## 1. INTRODUCTION

Thanks to the development of gamma-ray astronomy, the sample of GeV or TeV gamma-ray emitters is increasing. With the detection of high energy gamma-rays in over 60 blazars, such as 3C 279 and PKS 1510-089, in the GeV energy range by the EGRET experiment aboard the Compton Gamma Ray Observatory (Catanese et al. 1997; Fichtel et al. 1994; Lin et al. 1997; Mukherjee et al. 1997; Thompson et al. 1995, 1996; Villata et al. 1997), an exceptional opportunity presents itself for the understanding of the central engine operating in blazars. Some of blazars have been also firmly detected by atmospheric Cherenkov telescopes (ACTs) at energies above 1 TeV, such as Mrk 421 (Punch et al. 1992) and Mrk 501 (Quinn et al. 1996). The Large Area Telescope instrument on the Gamma-Ray Large Area Space Telescope (*GLAST*), the next-generation high energy gamma-ray telescope which will be launched next year, will observe gamma-rays with energies from 20 MeV to greater than 300 GeV, and have the unique capability to detect thousands of gamma-ray blazars to redshifts of at least  $z = 4$ , with sufficient angular resolution to allow identification of a large fraction of their optical counterparts (see e.g. Chen, Reyes, & Ritz 2004). The High Energy Stereoscopic System (HESS) is an imaging atmospheric Cherenkov detector dedicated to the ground based observation of gamma-rays at energies above 100 GeV (Funk et al. 2004; Hinton 2004; Hofmann 2003), and successfully detected TeV gamma-rays from many sources (see e.g. Aharonian et al. 2005). The Major Atmospheric Gamma Imaging Cherenkov telescope (MAGIC) is, currently the largest single-dish Imaging Air Cherenkov Telescope in operation, the one designed to have the lowest energy threshold of  $\sim 30$  GeV among the new Cherenkov telescopes (see e.g. Baixeras et al. 2004). The MAGIC telescope detected TeV gamma-rays from HESS J1813+178 (Albert et al. 2006). *GLAST*, combined with new-generation TeV instruments such as VERITAS, HESS and MAGIC, will tremendously improve blazar spectra studies, filling in the band from 20 MeV to 10 TeV with high significance data for hundreds of active galactic nuclei (AGNs) (see Gehrels & Michelson 1999). Future measurements of the gamma-ray spectra shape and its variability of blazars would tremendously improve our understanding to blazars.

Blazars are radio-loud AGNs characterized by luminous nonthermal continuum emission extending from radio up to GeV/TeV energies, very rapid variability, high and variable polarization, flat radio spectrum, high brightness temperatures and superluminal motion of compact radio cores (e.g. Urry & Padovani 1995). These unusual characteristics of blazars are generally believed to be attributed by emission from a relativistic jet oriented at a small angle to the line of sight (Blandford & Rees 1978). The spectral energy distributions of blazars consist of two broad bumps. The first component is from the synchrotron radiation processes. The second component is contributed by inverse Compton emission of the same electron population, including synchrotron self-Compton (SSC) scattering synchrotron seed

photons, and external Compton (EC) scattering seed photons from sources outside the jet (see e.g. Böttcher 1999). The external soft photon fields not only provide target photons for EC processes to produce the second component, but also absorb these gamma-rays from the EC processes, because gamma-rays with energies above 10 GeV interact with optical–UV photons and then could be attenuated by photon-photon pair production collisions with the external soft photons. The positions of gamma-ray emitting regions are still an open and controversial issue in the researches on blazars. It is suggested that gamma-rays are produced within broad line region (BLR) and that the gamma-ray emitting radius  $R_\gamma$  ranges roughly between 0.03 and 0.3 pc (Ghisellini & Madau 1996). It is argued by Georganopoulos et al. (2001) that the radiative plasma in relativistic jets of powerful blazars are within cavities formed by BLRs. However, it is also argued by other researchers that the gamma-ray emitting regions are outside BLRs (Lindfors, Valtaoja, & Turler 2005; Sokolov & Marscher 2005).

Observations found a large population of X-ray strong FSRQs, labeled HFSRQs by Perlman et al. (1998). HFSRQs have strong broad emission lines, flat hard X-ray spectra similar to classical FSRQs, but high synchrotron peak frequencies and steep soft X-ray spectra similar to intermediate or high synchrotron peak frequency BL Lac objects (e.g., Georganopoulos 2000; Padovani et al. 2003). Therefore, it is expected that HFSRQs are likely to be GeV–TeV gamma-ray emitters. For example, RGB J1629+4008 has a synchrotron peak  $\sim 2 \times 10^{16}$  Hz and a predicted Compton flux  $\nu F_\nu$  of nearly  $10^{-10}$  erg s $^{-1}$  cm $^{-2}$  at  $10^{25}$  Hz (Padovani et al. 2002). However, the BLRs can reprocess and scatter the central UV radiation to produce diffuse line emission and continuum radiation, respectively. The two external diffuse radiation could absorb gamma-rays with energies from 10 to 200 GeV. Then, it is unknown whether these gamma-rays could be detected by *GLAST* even if blazars intrinsically produce gamma-rays with energies from 10 to 200 GeV in the observer’s frame. In this paper, we focus our efforts on the photon-photon absorption for these gamma-rays by the two diffuse radiation fields of the BLRs in the powerful blazars, and then hope to limit constraints on the positions of gamma-ray emitting regions by comparing our results with *GLAST* observations in the near future.

The structure of this paper is as follows. Section 2 consists of four subsections, in which subsection 2.1 presents the cross section of pair production, subsection 2.2 the photon-photon attenuation optical depth, subsection 2.3 the diffuse radiation field of the BLR, and subsection 2.4 the dependence of  $\tau_{\gamma\gamma}$  on parameters. Section 3 presents the photon-photon absorption optical depth for FSRQs, section 4 presents applications to individual sources, and the last section is for discussions and conclusions. Throughout this paper, we use a flat cosmology with a deceleration factor  $q_0 = 0.5$  and a Hubble constant  $H_0 = 75$  km s $^{-1}$  Mpc $^{-1}$ .

## 2. THEORETICAL CALCULATION

### 2.1. The Cross Section of Pair Production

Gamma-ray photons can be absorbed by the photo-annihilation/pair creation process  $\gamma + \gamma \rightarrow e^+ + e^-$ , for which the total cross section is (e.g., Gould & Schreder 1967; Jauch & Rohrlich 1976):

$$\sigma(x) = \frac{3\sigma_T}{16}(1-x^2) \left[ (3-x^4) \ln \frac{1+x}{1-x} - 2x(2-x^2) \right], \quad (1)$$

where  $\sigma_T$  is the Thomson cross section, and  $x$  is the velocity of the pairs in the center of moment system and defined as

$$x \equiv \sqrt{1 - \frac{2}{\frac{h\nu_1}{m_e c^2} \frac{h\nu_2}{m_e c^2} (1 - \cos \theta)}} = \sqrt{1 - \frac{2}{\varepsilon_1 \varepsilon_2 (1 - \mu)}}, \quad (2)$$

where  $h$  is the Plank constant,  $m_e$  the rest mass of electron,  $c$  the speed of light,  $\varepsilon_1$  ( $\varepsilon_2$ ) is the energy of the high (low) energy photon in units of the rest mass energy of electron, and  $\mu$  is the cosine of the collision angle  $\theta$  (Coppi & Blandford 1990). The threshold condition of photon-photon pair creation process is

$$\frac{1}{2} \varepsilon_1 \varepsilon_2 (1 - \cos \theta) \geq 1. \quad (3)$$

The total cross section reaches the maximum value with  $\sigma_{\max} \approx 0.26\sigma_T$  at  $x \approx 0.7$ , which corresponds to

$$\varepsilon_1 \varepsilon_2 (1 - \cos \theta) \approx 4. \quad (4)$$

Then we have  $\varepsilon_1 \varepsilon_2 \gtrsim 2$  because  $0 \leq \theta \leq \pi$ . For the  $\gamma - \gamma$  attenuation process, only the photons with the product  $\varepsilon_1 \varepsilon_2 \gtrsim 2$  could have the maximum cross section  $\sigma_{\max} \approx 0.26\sigma_T$ .

### 2.2. The $\gamma - \gamma$ Attenuation Optical Depth

The  $\gamma - \gamma$  attenuation optical depth per unit length  $dl$  at distance  $R$  from the central black hole along the direction of jet axis is

$$\frac{d}{dl} \tau_{\gamma\gamma}(\varepsilon_1, R) = \int \int \int \sigma(x) n_{\text{ph}}(R, \varepsilon_2, \Omega) (1 - \mu) d\varepsilon_2 d\Omega, \quad (5)$$

where  $n_{\text{ph}}(R, \varepsilon_2, \Omega)$  is the number density of soft photon at the position  $R$  per unit frequency range per unit solid angle. For these gamma-rays produced at the position of  $R_\gamma$  along the

jet axis, the  $\gamma - \gamma$  attenuation optical depth is

$$\tau_{\gamma\gamma}(\varepsilon_1) = \int_{R_\gamma}^{\infty} \frac{d}{dl} \tau_{\gamma\gamma}(\varepsilon_1, R) dR, \quad (6)$$

and the escape probability of gamma photons of  $\varepsilon_1$ ,  $P_{\text{esc}}(\varepsilon_1)$ , is

$$P_{\text{esc}}(\varepsilon_1) = e^{-\tau_{\gamma\gamma}(\varepsilon_1)}. \quad (7)$$

In next paragraphs, we calculate the energy density distribution of gamma-ray absorbing photons from both scattering and reprocessing, and then estimate the  $\gamma - \gamma$  attenuation optical depth.

First, we calculate the intensity by integrating the emissivity along lines of sight through BLR, which is assumed as a spherical shell of clouds with the outer radius  $r_{\text{BLR,out}}$  and the inner radius  $r_{\text{BLR,in}}$  (see Fig. 1). A fraction  $df_{\text{cov}}(r) = n_c(r)\sigma_c(r)dr$  of the central UV luminosity  $L_{\text{UV}}$  would then be reprocessed into emission lines in  $r \rightarrow r + dr$ , where  $n_c(r)$  and  $\sigma_c(r)$  are the number density and the cross section of clouds at radius  $r$ , respectively. Since a thin spherical shell has volume  $4\pi r^2 dr$ , the emissivity (in  $\text{erg s}^{-1} \text{cm}^{-3} \text{ster}^{-1}$ ) of reprocessed radiation inside the BLR at the radius  $r$  is

$$j_{\text{line}}(r) = \frac{L_{\text{UV}} df_{\text{cov}}}{16\pi^2 r^2 dr} = \frac{L_{\text{UV}} n_c \sigma_c}{16\pi^2 r^2}, \quad (8)$$

where  $\sigma_c = \pi R_c^2$  and  $R_c$  is the radius of clouds at the radius  $r$ . For  $n_c = n_{c0}(r/r_{\text{BLR,in}})^{-p}$  and  $R_c = R_{c0}(r/r_{\text{BLR,in}})^q$ , where  $n_{c0}$  and  $R_{c0}$  is the number density and the radius of clouds at  $r_{\text{BLR,in}}$ , respectively, the covering factor  $f_{\text{cov}}$  of the entire BLR to the central UV radiation is

$$f_{\text{cov}} = \int_{r_{\text{BLR,in}}}^{r_{\text{BLR,out}}} n_{c0} \pi R_{c0}^2 \left( \frac{r}{r_{\text{BLR,in}}} \right)^{2q-p} dr. \quad (9)$$

In this paper, we adopt the power law exponents preferred by Kaspi & Netzer (1999),  $q = 1/3$  and  $p = 1.5$ . The central UV radiation is also scattered by the BLR clouds into the diffuse continuum, and the diffuse soft photons can absorb gamma-rays with energies above 10 GeV. A fraction  $d\tau_{\text{BLR}} = n_e \sigma_T dr$  of the central UV luminosity would then be scattered in  $r \rightarrow r + dr$ , where  $n_e$  is the number density of electrons in the BLR clouds at the radius  $r$ . Since this spherical shell has volume  $4\pi r^2 dr$ , the emissivity of scattered radiation inside the BLR at the radius  $r$  is

$$j_{\text{cont}}(r) = \frac{L_{\text{UV}} d\tau_{\text{BLR}}}{16\pi^2 r^2 dr} = \frac{L_{\text{UV}} n_e \sigma_T}{16\pi^2 r^2}, \quad (10)$$

if the Thomson optical depth of the BLR  $\tau_{\text{BLR}} \ll 1$ . For  $n_e = n_{e0}(r/r_{\text{BLR,in}})^{-s}$ , where  $n_{e0}$  is the number density of electrons in the BLR clouds at  $r_{\text{BLR,in}}$ , the Thomson optical depth of

the entire BLR to the central UV radiation is

$$\tau_{\text{BLR}} = \int_{r_{\text{BLR},\text{in}}}^{r_{\text{BLR},\text{out}}} n_{\text{e}0} \sigma_{\text{T}} \left( \frac{r}{r_{\text{BLR},\text{in}}} \right)^{-s} dr. \quad (11)$$

In this paper, we adopt the power law exponent preferred by Kaspi & Netzer (1999),  $s = 1$ . From equations (8) and (9) and the relation of the luminosity of broad emission lines from the BLR and the central UV luminosity  $L_{\text{BLR}} = f_{\text{cov}} L_{\text{UV}}$  (D’Elia et al. 2003), we get the expression for the diffuse line emission

$$j_{\text{line}}(r) = \frac{L_{\text{BLR}} r^{2q-p-2}}{16\pi^2 \int_{r_{\text{BLR},\text{in}}}^{r_{\text{BLR},\text{out}}} r^{2q-p} dr}. \quad (12)$$

From equations (10) and (11) and  $L_{\text{BLR}} = f_{\text{cov}} L_{\text{UV}}$ , we also get the emissivity for the diffuse continuum radiation

$$j_{\text{cont}}(r) = \frac{L_{\text{BLR}} \tau_{\text{BLR}} r^{-s-2}}{16\pi^2 f_{\text{cov}} \int_{r_{\text{BLR},\text{in}}}^{r_{\text{BLR},\text{out}}} r^{-s} dr}. \quad (13)$$

The intensity of radiation with angle  $\theta$  to the jet axis at a position  $R$  is given by

$$I(R, \theta) = \int_0^{l_{\text{max}}} j(r) dl, \quad (14)$$

where  $j(r)$  represents  $j_{\text{cont}}(r)$ ,  $j_{\text{line}}(r)$  or  $j_{\text{cont}}(r) + j_{\text{line}}(r)$ , and vanishes when  $r > r_{\text{BLR},\text{out}}$  or  $r < r_{\text{BLR},\text{in}}$ . We can get the following relations from the triangle in Figure 1

$$r^2 = R^2 - 2Rl \cos \theta + l^2, \quad (15)$$

$$l_{\text{max}} = R \cos \theta + R \sqrt{\cos^2 \theta + \left( \frac{r_{\text{BLR},\text{out}}}{R} \right)^2} - 1. \quad (16)$$

The energy density of radiation from the BLR is expressed as

$$U(R) = \int \int \frac{I(R, \theta)}{c} d\Omega = \frac{2\pi}{c} \int_0^\pi I(R, \theta) \sin \theta d\theta, \quad (17)$$

and is a function of distance  $R$  from the center along the direction of the jet axis.

### 2.3. The Diffuse Radiation Field of BLR

Though, the emission lines  $Ly\alpha$ ,  $CIV$ ,  $MgII$ ,  $H_\gamma$ ,  $H_\beta$  and  $H_\alpha$  are the major contributors to the total broad line emission, the contributions from all the emission lines reported by Francis et al. (1991) and the emission line  $H_\alpha$  reported by Gaskell et al. (1981) are included

to estimate the total flux of broad emission lines,  $F_{\text{BLR}}$ . Together 35 components of emission lines are considered to estimate the total flux of broad emission lines. The sum of line ratios  $N_\nu$ , relative to the  $Ly\alpha$  with a reference value of  $N_\nu = 100$ , of all the 35 components of emission lines is equal to 555.77 (Francis et al. 1991). The relative intensities of the 35 components of emission lines are presented in Figure 3. It is assumed that the flux of a certain emission line is equal to

$$F_\nu = \frac{N_\nu}{555.77} F_{\text{BLR}}. \quad (18)$$

According to the definition of flux, we have relations of  $F_{\text{BLR}} = \int I_{\text{line}}(R, \theta) \cos \theta d\Omega$  and  $F_\nu = \int I(R, \nu, \theta) \cos \theta d\Omega$ . Comparing the two relations with equation (18), we have a relation of  $I(R, \nu, \theta) = N_\nu I_{\text{line}}(R, \theta)/555.77$  between the total intensity  $I_{\text{line}}(R, \theta)$  and the monochromatic intensity  $I(R, \nu, \theta)$  for the emission line. Then the photon number density of the emission line along the direction of  $\theta$  at the position of  $R$  is

$$n_{\text{ph}}(R, \nu, \Omega) = \frac{I(R, \nu, \theta)}{h\nu c} = \frac{N_\nu}{555.77} \frac{I_{\text{line}}(R, \theta)}{h\nu c}. \quad (19)$$

A diluted blackbody spectrum at the position of  $R$  along the direction of  $\theta$  is assumed for the diffuse continuum as

$$n_{\text{ph}}(R, \nu, \Omega) = \frac{2n(R, \theta)\nu^2}{c^3 [\exp(\frac{h\nu}{kT}) - 1]} = n(R, \theta)n_{\text{bb}}(\nu, T), \quad (20)$$

where  $k$  is the Boltzmann constant, and  $n(R, \theta)$  is the normalization factor to a blackbody spectrum  $n_{\text{bb}}(\nu, T)$  and can be calculated by the formula

$$n(R, \theta) = \frac{I_{\text{cont}}(R, \theta)}{c \int_{\nu_2^L}^{\nu_2^U} n_{\text{bb}}(\nu, T) h\nu d\nu}, \quad (21)$$

because  $I_{\text{cont}}(R, \theta) = cn(R, \theta) \int n_{\text{bb}}(\nu, T) h\nu d\nu$ . In the calculations of the  $\gamma - \gamma$  attenuation optical depth, the soft photon frequency is considered in the range from  $\nu_2^L = 10^{14.6}$  Hz to  $\nu_2^U = 10^{16.5}$  Hz for the diffuse continuum at the bands of the optical to UV, and the blackbody temperature  $T = 10^5$  K is assumed for the inner regions of the accretion disk.

#### 2.4. The Dependence of $\tau_{\gamma\gamma}$ on Parameters

According to the interpretation of the data obtained in many reverberation campaigns, production of broad emission lines in quasars is peaked around some distance (see Peterson 1993; Kaspi 2000; Sulentic et al. 2000). Wu et al. (2004) derived an empirical relation between the BLR size  $r_{\text{BLR}}$  deduced from the reverberation mapping and  $H_\beta$  luminosity

$$\log r_{\text{BLR}} = -1.695 + 0.684 \log \frac{L_{H_\beta}}{10^{42} \text{ erg s}^{-1}} \text{ pc}. \quad (22)$$

From equation (18) and the line ratio of  $N_\nu = 22$  for the emission line  $H_\beta$ , the empirical relation is also expressed as

$$r_{\text{BLR}} = 0.250 \times \left( \frac{L_{\text{BLR}}}{10^{45} \text{ erg s}^{-1}} \right)^{0.684} \text{ pc} = 0.250 L_{\text{BLR},45}^{0.684} \text{ pc}, \quad (23)$$

where  $L_{\text{BLR},45} = L_{\text{BLR}}/(10^{45} \text{ erg s}^{-1})$ . We assume that the distance  $r_{\text{BLR}}$  deduced from equation (23) represents the median of  $r_{\text{BLR},\text{in}}$  and  $r_{\text{BLR},\text{out}}$ , that is,  $r_{\text{BLR},\text{in}} = r_{\text{BLR}} - h$  and  $r_{\text{BLR},\text{out}} = r_{\text{BLR}} + h$ , where  $h$  is the half thickness of the spherical shell of clouds.

We derived an average broad line luminosity of  $L_{\text{BLR}} = 10^{45.35} \text{ erg s}^{-1}$  for 25 FSRQs from Cao & Jiang (1999), and took it as the typical value of  $L_{\text{BLR}}$  for powerful blazars. The typical value of  $L_{\text{BLR}} = 10^{45.35} \text{ erg s}^{-1}$  for FSRQs corresponds to a distance  $r_{\text{BLR}} \simeq 0.43 \text{ pc}$ . In order to illustrate the radial dependence of the energy density of the diffuse radiation on the two parameters  $r_{\text{BLR}}$  and  $h$ , equivalently  $r_{\text{BLR},\text{in}}$  and  $r_{\text{BLR},\text{out}}$ , we firstly consider four cases with four values of  $h$  at a fixed  $r_{\text{BLR}} = 0.43 \text{ pc}$ , and then consider four cases with four values of  $r_{\text{BLR}}$  at a fixed  $h = 0.20 \text{ pc}$  by assuming a ratio  $\tau_{\text{BLR}}/f_{\text{cov}} = 1$ . The relevant energy density distributions of the diffuse radiation fields are plotted in Figure 2. It can be seen that for each case the energy density peaks around the inner radius  $r_{\text{BLR},\text{in}}$ , and decreases rapidly beyond the outer radius  $r_{\text{BLR},\text{out}}$ . On the whole, the energy density inside the inner radius increases as the parameter  $h$  increases for a fixed  $r_{\text{BLR}}$ , and the average energy density inside the outer radius also increases as  $h$  increases. The energy density inside the inner radius decreases as the parameter  $r_{\text{BLR}}$  increases for a fixed  $h$ , and the average inside the outer radius also decreases as  $r_{\text{BLR}}$  increases. The energy density outside the inner radius does not monotonously increase with  $h$  for a fixed  $r_{\text{BLR}}$  (see Fig. 2c). At a fixed  $r_{\text{BLR}}$ , the increasing of  $h$  results in the increasing of  $r_{\text{BLR},\text{out}}$  and decreasing of  $r_{\text{BLR},\text{in}}$ . It can be seen from Figure 2c that the variation of the inner radius can significantly change the energy density distributions, but the energy density distributions slightly alter as the outer radius changes. At a fixed  $h$ , the increasing of  $r_{\text{BLR}}$  results in the increasing of  $r_{\text{BLR},\text{in}}$  and  $r_{\text{BLR},\text{out}}$ . It is obvious that the energy density tends to become smaller as either  $r_{\text{BLR},\text{in}}$  or  $r_{\text{BLR},\text{out}}$  becomes larger (see Fig. 2a, b). The energy density outside the inner radius does not monotonously decrease with  $r_{\text{BLR}}$  for a fixed  $h$  (see Fig. 2a, b). In addition, the radial dependencies of the energy densities have a very similar behavior as  $R$  is large enough. In order to study the dependence of  $\tau_{\gamma\gamma}$  on parameters  $h$ ,  $R_\gamma$  and  $r_{\text{BLR}}$ , a ratio of  $\tau_{\text{BLR}}/f_{\text{cov}} = 1$  is assumed and the BLR luminosity of  $L_{\text{BLR}} = 10^{45.35} \text{ erg s}^{-1}$  is adopted for FSRQs.

We assume  $R_\gamma = r_{\text{BLR}}$  and take four values of  $h$  to study the dependence of the photon-photon absorption optical depth on the parameter  $h$ . The calculated results are presented in Figure 4. The parameter  $h$  influences the photon-photon absorption optical depth, but the influence of  $h$  on the calculated results is not very important (see Fig. 4a). It can

be seen from Figure 4a that the optical depth  $\tau_{\gamma\gamma}$  does not monotonously increase with  $h$ , qualitatively changing the dependence on  $h$  with  $E_\gamma$ . We study the dependence of  $\tau_{\gamma\gamma}$  on  $h$  for four values of  $E_\gamma$  to check if this effect is real. The calculated results are presented in Figure 4b, and we can see from Figure 4b that the optical depth  $\tau_{\gamma\gamma}$  does not monotonously increase with  $h$ , qualitatively changing the dependence on  $h$  with  $E_\gamma$ . To better show this effect, we normalize  $\tau_{\gamma\gamma}(h)$  by the factor  $\tau_{\gamma\gamma}(0.05 \text{ pc})$  for the four curves in Figure 4b, and the normalized results are presented in Figure 4c. For the curves I, II and III with the relevant  $E_\gamma$  at 50, 100 and 150 GeV, the optical depth  $\tau_{\gamma\gamma}$  at four  $h$  have an order of  $\tau_{\gamma\gamma}(0.05 \text{ pc}) < \tau_{\gamma\gamma}(0.30 \text{ pc}) < \tau_{\gamma\gamma}(0.20 \text{ pc}) < \tau_{\gamma\gamma}(0.15 \text{ pc})$  (see Fig. 4c). For the curve I+II with  $E_\gamma$  at 200 GeV, the optical depth  $\tau_{\gamma\gamma}$  at four  $h$  have a sequence of  $\tau_{\gamma\gamma}(0.30 \text{ pc}) < \tau_{\gamma\gamma}(0.05 \text{ pc}) < \tau_{\gamma\gamma}(0.20 \text{ pc}) < \tau_{\gamma\gamma}(0.15 \text{ pc})$  (see Fig. 4c). It is obvious that the optical depth  $\tau_{\gamma\gamma}$  does not monotonously increase with  $h$  and the dependence of  $\tau_{\gamma\gamma}$  on  $h$  qualitatively changes with  $E_\gamma$  (see Fig. 4c). Then this effect is real, and it could result from several factors. Though, the energy density inside the inner radius and the average energy density increase as  $h$  increases for a fixed  $r_{\text{BLR}}$ , a majority of the diffuse radiation cannot make a contribution to the optical depth  $\tau_{\gamma\gamma}$  because of the assumption of  $R_\gamma = r_{\text{BLR}}$ . Only the diffuse radiation outside  $r_{\text{BLR}}$  can make a contribution to the optical depth  $\tau_{\gamma\gamma}$ , and then this results in the non-monotonous dependence of  $\tau_{\gamma\gamma}$  on  $h$  at a fixed  $r_{\text{BLR}}$  because the energy density distributions outside  $r_{\text{BLR}}$  do not monotonously increase with  $h$ . Only the fraction of soft photons matching the threshold condition can make a contribution to the photon-photon absorption, and this makes a contribution to the non-monotonous dependence on  $h$ . These factors together result in this effect that the optical depth  $\tau_{\gamma\gamma}$  does not monotonously increase with  $h$ , qualitatively changing the dependence on  $h$  with  $E_\gamma$ . If  $R_\gamma = r_{\text{BLR, in}}$ , the dependence on  $h$  at a fixed  $r_{\text{BLR}}$  could be monotonous because more absorption with  $h$  increasing can be contributed by the diffuse radiation between  $r_{\text{BLR, in}}$  and  $r_{\text{BLR}}$ , and this is justified by the photon-photon absorption for HFSRQ PKS 0405–123 in Figure 8 (see section 4).

In order to study the dependence of  $\tau_{\gamma\gamma}$  on the parameter  $R_\gamma$ , we adopt  $r_{\text{BLR}} = 0.43 \text{ pc}$  and assume the half thickness of BLR  $h = 0.20 \text{ pc}$ . The calculated results with four values of  $R_\gamma$  are presented in Figure 5. The farther the gamma-ray emitting region from the central black hole, the less the absorption optical depth of gamma-rays. When the gamma-ray emitting region is close to the outer radius of BLR, the two diffuse radiation fields we concerned are transparent for gamma-rays with energies from 10 to 200 GeV. If the gamma-ray emitting region is close to the inner radius of BLR, the two diffuse radiation fields we concerned are not transparent for gamma-rays between 10 and 200 GeV. This trend of the absorption optical depth in Figure 5 can be easily explained from the energy density distributions in Figure 2. The closer the gamma-ray emitting region to the center of

BLR, the larger the displacement of the escaping gamma-rays and the more the gamma-ray absorbing photons. The absorption optical depth  $\tau_{\gamma\gamma}$  rapidly decreases as the parameter  $R_\gamma$  increases. The photon field energy density sharply reduces as  $R_\gamma > r_{\text{BLR,in}}$ , and this makes the absorption optical depth  $\tau_{\gamma\gamma}$  rapidly reduce.

We take four values of  $r_{\text{BLR}}$  to study the dependence of the absorption optical depth  $\tau_{\gamma\gamma}$  on the parameter  $r_{\text{BLR}}$ . In the calculations, it is supposed that  $R_\gamma = r_{\text{BLR}}$  and  $h = 0.20$  pc. The calculated results are presented in Figure 6. It can be seen in Figure 6 that the optical depth  $\tau_{\gamma\gamma}$  slowly reduces as the parameter  $r_{\text{BLR}}$  increases. This trend of the absorption optical depth can be also easily explained from the energy density distributions in Figure 2. The increasing of BLR scale  $r_{\text{BLR}}$  makes the inner and outer radii of BLR become larger, and this results in the decreasing of the energy density of radiation fields we concerned, and then the decreasing of the optical depth of photon-photon absorption.

### 3. THE PHOTON-PHOTON ABSORPTION OPTICAL DEPTH FOR FSRQs

According to Ghisellini et al. (1998), for FSRQs, the Lorentz factors have the typical value of  $\Gamma \sim 15$ , the magnetic energy densities are on the order of  $U'_B \sim 0.1$  erg cm<sup>-3</sup> measured in the blob comoving frame, and the Compton dominance of  $L_{\text{EC}}/L_{\text{Syn}}$  is  $\sim 20$ , where  $L_{\text{EC}}$  is the EC luminosity and  $L_{\text{Syn}}$  the synchrotron luminosity. It is suggested that there are relations of  $L_{\text{EC}} \gg L_{\text{SSC}}$  and  $L_{\text{EC}}/L_{\text{Syn}} \simeq 20$  for FSRQs on average, where  $L_{\text{SSC}}$  is the SSC luminosity (Georganopoulos et al. 2001). This Compton dominance  $L_{\text{EC}}/L_{\text{Syn}} \simeq 20$  is consistent with the result of Ghisellini et al. (1998). There is a relationship of  $L_{\text{EC}}/L_{\text{Syn}} \simeq U'_{\text{ph}}/U'_B = U_{\text{ph}}/U_B$  between the ratio of EC to synchrotron luminosity and the ratio of external radiation energy density  $U_{\text{ph}}$  to magnetic energy density  $U_B$  for powerful blazars. The external radiation energy densities of FSRQs have a typical value of  $U_{\text{ph}} \simeq U_B L_{\text{EC}}/L_{\text{Syn}} \simeq \Gamma^{-2} U'_B L_{\text{EC}}/L_{\text{Syn}} \sim 10^{-2.1}$  erg cm<sup>-3</sup>. Assuming the ratio of  $\tau_{\text{BLR}}/f_{\text{cov}}$  on the order of unity, the calculations indicate that the average of the external radiation energy densities within the outer radius  $r_{\text{BLR,out}}$  is on the order of  $\bar{U}_{\text{ph}} \sim 10^{-2.1}$  erg cm<sup>-3</sup> as  $r_{\text{BLR,in}} \sim 0.2$  pc and  $r_{\text{BLR,out}} \sim 0.6$  pc. The median of the probable positions of inner and outer radii is around 0.4 pc, which is in well agreement with  $r_{\text{BLR}} \simeq 0.43$  pc derived from equation (23) and the typical value of  $L_{\text{BLR}} = 10^{45.35}$  erg s<sup>-1</sup> for FSRQs. This agreement implies it reasonable that we adopt the value of  $r_{\text{BLR}}$  derived from equation (23) as the median of  $r_{\text{BLR,in}}$  and  $r_{\text{BLR,out}}$  for FSRQs. The typical values of  $L_{\text{BLR}} = 10^{45.35}$  erg s<sup>-1</sup> and  $U_{\text{ph}} \sim 10^{-2.1}$  erg cm<sup>-3</sup> for FSRQs limit the probable positions of inner and outer radii of BLR around 0.2 pc and 0.6 pc, respectively, and also confine the half thickness of BLR about

$h \sim 0.20$  pc. Then, we adopt  $r_{\text{BLR}} \simeq 0.43$  pc and  $h \sim 0.20$  pc to estimate the photon-photon absorption optical depth of gamma-rays with energies from 10 to 200 GeV for FSRQs.

However, the gamma-ray emitting regions are still a controversial issue in the studies on blazars. It has been suggested that gamma-rays are produced within the BLR, and the gamma-ray emitting radius  $R_\gamma$  ranges roughly between 0.03 and 0.3 pc (Ghisellini & Madau 1996). The radiative plasma in the relativistic jets of the powerful blazars are within the BLR cavities (Georganopoulos et al. 2001), and then there are  $R_\gamma \lesssim r_{\text{BLR, in}}$  for FSRQs with the typical value of  $L_{\text{BLR}} = 10^{45.35}$  erg s<sup>-1</sup>. Based on the dependence of  $\tau_{\gamma\gamma}$  on the parameter  $R_\gamma$  discussed in previous section, the closer the gamma-ray emitting regions to the central black holes, the larger the optical depth of photon-photon absorption, and then we adopt  $R_\gamma \sim r_{\text{BLR, in}}$  to estimate the  $\gamma - \gamma$  absorption optical depth of gamma-rays with energies from 10 to 200 GeV. Assuming for FSRQs that  $R_\gamma \sim r_{\text{BLR, in}}$ ,  $h \sim 0.20$  pc and  $L_{\text{BLR}} = 10^{45.35}$  erg s<sup>-1</sup> corresponding to  $r_{\text{BLR}} \simeq 0.43$  pc, we estimate the photon-photon absorption optical depth of gamma-rays between 10 and 200 GeV. The line emission is completely transparent to gamma-rays below 30 GeV (see Fig. 7), because the threshold condition of photon-photon pair creation process cannot be satisfied between these gamma-rays below 30 GeV and the emission lines listed in Figure 3. However, the diluted blackbody radiation is not transparent to these gamma-rays below 30 GeV (see Fig. 7). On the other hand, the emission lines contribute much more than the diluted blackbody radiation to the absorption for gamma-rays with energies from  $\sim 50$  to 200 GeV. Even if the diluted blackbody radiation is not considered in the calculations, the line emission is not transparent to these gamma-rays with energies from  $\sim 50$  to 200 GeV (see Fig. 7). Then, gamma-rays with energies from 10 to 200 GeV cannot escape from the emission line and diluted blackbody radiation fields of the BLRs in FSRQs as long as  $R_\gamma \lesssim r_{\text{BLR, in}}$  (see Fig. 7). In this section, the redshift effect is not considered for gamma-rays with energies from 10 to 200 GeV in the observed spectrum, and this effect will be considered for individual sources in the following section.

#### 4. APPLICATION TO INDIVIDUAL SOURCES

The discovery of a large population of X-ray strong FSRQs (labeled HFSRQs by Perlman et al. 1998) gives a fundamental change in our perception of the broadband spectra of FSRQs. HFSRQs have strong broad emission lines, flat hard X-ray spectra similar to classical FSRQs, but high synchrotron peak frequency and steep soft X-ray spectra similar to intermediate or high synchrotron peak frequency BL Lac objects, and are classified as a new subclass of blazars (e.g., Georganopoulos 2000; Padovani et al. 2003). An example of such an object

is RGB J1629+4008 with a synchrotron peak  $\sim 2 \times 10^{16}$  Hz and a predicted flux  $\nu F_\nu$  of nearly  $10^{-10}$  erg s $^{-1}$  cm $^{-2}$  at  $10^{25}$  Hz (Padovani et al. 2002). Therefore, HFSRQs are likely to be GeV–TeV gamma-ray emitters with the Compton peak energies possibly from multi-ten to multi-hundred GeV. A powerful HFSRQ with  $L_{\text{BLR}}$  obtained in literature is PKS 0405–123, and it has a BLR luminosity  $L_{\text{BLR}} = 10^{45.67}$  erg s $^{-1}$  and redshift  $z = 0.574$  (e.g., Georganopoulos 2000). Assuming that HFSRQs have the same properties of BLRs as the classical FSRQs, we estimate the optical depth of photon-photon absorption for the strong-lined, powerful HFSRQ PKS 0405–123. In the calculations, we assume  $R_\gamma \sim r_{\text{BLR},\text{in}}$  and  $\tau_{\text{BLR}}/f_{\text{cov}} = 1$ , and take three values of  $h$ , because it is unclear whether the parameter  $h$  equals  $\sim 0.20$  pc for PKS 0405–123. From Figure 8 we see that the two diffuse radiation fields of BLR are not transparent to gamma-rays with energies from 10 to 200 GeV in the observed spectrum for this powerful HFSRQ as long as  $R_\gamma \lesssim r_{\text{BLR},\text{in}}$ . If *GLAST* detect gamma-rays with energies from 10 to 200 GeV emitted by PKS 0405–123, either the gamma-ray emitting regions are not within the BLR cavity or the model used and the relevant assumptions made in this paper are incorrect.

The classical FSRQ 3C 279,  $z = 0.536$ , is one of the brightest extragalactic objects in the gamma-ray sky, and has a BLR luminosity  $L_{\text{BLR}} = 10^{44.41}$  erg s $^{-1}$  (Cao & Jiang 1999). It was detected by the EGRET in the 0.1–10 GeV energy domain, and its spectrum above  $\sim 100$  MeV can be fitted by a power law and do not show any signature of gamma-ray absorption by pair production up to  $\sim 10$  GeV (Fichtel et al. 1994; von Montigny et al. 1995). We calculate the optical depth to photon-photon absorption for 3C 279 by adopting  $r_{\text{BLR},\text{in}} = 0.1$  pc and  $r_{\text{BLR},\text{out}} = 0.4$  pc from Hartman et al. (2001) and assuming  $R_\gamma \sim r_{\text{BLR},\text{in}}$ . The photon-photon absorption optical depth is presented by the dashed curve in Figure 8. It can be seen in Figure 8 that the diffuse radiation fields are not transparent to gamma-rays with energies around 10 GeV, and this result is not consistent with the observations (e.g., Fichtel et al. 1994; von Montigny et al. 1995; Ghisellini & Madau 1996; Wehrle et al. 1998). There are two probable factors that make the optical depth overestimated. The first one is the assumption of  $R_\gamma \sim r_{\text{BLR},\text{in}}$  that can lead to the overestimation of  $\tau_{\gamma\gamma}$ . The second one is the assumption of  $\tau_{\text{BLR}}/f_{\text{cov}} = 1$  that can also result in the same consequence as the first one. If  $\tau_{\text{BLR}}/f_{\text{cov}} = 1/3$ , the photon-photon absorption optical depth of these gamma-rays around 10 GeV is less than unity, and the two diffuse radiation fields are optically thick to these gamma-rays in the interval between multi-ten and 200 GeV. *GLAST* observations in the future could limit strong constraints on the position of the gamma-ray emitting region relative to the inner radius of BLR and the BLR properties for 3C 279.

## 5. DISCUSSIONS AND CONCLUSIONS

It can be seen from equation (12) that the emissivity of emission lines is unrelated to the covering factor, and then the relevant absorption for gamma-rays is also unrelated with the value of  $f_{\text{cov}}$ . The gamma-ray absorption contributed by the diluted blackbody radiation is in proportion to the ratio  $\tau_{\text{BLR}}/f_{\text{cov}}$  (see eq. 13). There is a large uncertainty in the BLR covering factor, and the uncertainty could affect our results. Early estimates of this quantity indicated a covering factor  $f_{\text{cov}} \sim 5 - 10\%$ , while recent observations indicated instead  $f_{\text{cov}} \sim 30\%$  (e.g., Maiolino et al. 2001). Estimates of the BLR covering factors need to measure UV continuum emission from accretion disks. In the case of blazars, these UV continuum emission are swamped by the beaming components from relativistic jets, and this makes it difficult to calculate the BLR covering factors for blazars. The way out to roughly estimate  $f_{\text{cov}}$  is to know the BLR luminosity  $L_{\text{BLR}}$  of blazars, in which the thermal emission is clearly dominating the synchrotron ones. D’Elia et al. (2003) found only two of these blazars in literatures: 3C 273 and PKS 2149-306. They obtained  $f_{\text{cov}} \sim 7\%$  for the first source, while  $f_{\text{cov}} \sim 10\%$  for the second one. D’Elia et al. (2003) adopted the BLR covering factor  $f_{\text{cov}} \sim 10\%$  as the typical value of  $f_{\text{cov}}$  for their blazar sample. Donea & Protheroe (2003) suggested  $f_{\text{cov}} \sim 3\%$  for the spherical distribution of the BLR clouds in quasars. The issue of the Thomson optical depth of BLRs has been rarely studied and has gotten nowhere for blazars. Blandford & Levison (1995) adopted the Thomson optical depth of BLR as  $\tau_{\text{BLR}} = 0.01$ . Then the ratio  $\tau_{\text{BLR}}/f_{\text{cov}}$  of the Thomson optical depth to the covering factor is likely to be typically of  $\tau_{\text{BLR}}/f_{\text{cov}} \sim 1/3$  for the spherical distribution of the BLR clouds in blazars. This value of  $\tau_{\text{BLR}}/f_{\text{cov}} \sim 1/3$  is on the same order of magnitude as  $\tau_{\text{BLR}}/f_{\text{cov}} = 1$ , assumed in the previous sections.

As stated in section 3, the external radiation energy densities of FSRQs are on the order of  $U_{\text{ph}} \sim 10^{-2.1} \text{ erg cm}^{-3}$ , and this typical value limits constraints on the probable positions of inner and outer radii of BLR or the half thickness of spherical shell of BLR. The probable positions of the inner and outer radii are around  $r_{\text{BLR, in}} \sim 0.2 \text{ pc}$  and  $r_{\text{BLR, out}} \sim 0.6 \text{ pc}$ , respectively. The median of this probable inner and outer radii is around  $0.4 \text{ pc}$ , which is consistent with the radius  $r_{\text{BLR}} \simeq 0.43 \text{ pc}$  derived from the reverberation mapping. This agreement implies that the radius  $r_{\text{BLR}}$  derived from the reverberation mapping probably denotes the median of  $r_{\text{BLR, in}}$  and  $r_{\text{BLR, out}}$ , and our assumption of  $r_{\text{BLR}}$  in the previous sections is appropriate. The energy density distribution for the BLR with  $r_{\text{BLR, in}} \sim 0.2 \text{ pc}$ ,  $r_{\text{BLR, out}} \sim 0.6 \text{ pc}$  and  $\tau_{\text{BLR}}/f_{\text{cov}} \sim 1/3$  has an average of energy densities within the outer radius on the order of  $U_{\text{ph}} \sim 10^{-2.1} \text{ erg cm}^{-3}$ . The corresponding absorption optical depth for gamma-rays is presented by the curve III in Figure 7, from which it can be seen that the two diffuse radiation fields of the BLRs are not transparent to these gamma-rays with energies from 10 to 200 GeV.

Because of the relativistic beaming effect, most of gamma-rays for FSRQs are contained within a radiation cone with a half open angle of  $\Delta\varphi \sim 1/\Gamma \sim 3.8^\circ$ . If the central UV photons directly from accretion disks travel through the radiation cone, the UV photons can have photon-photon pair creation processes with gamma-rays within the radiation cone. Assuming the radius of the UV radiation region is around  $R_D \sim 100R_s \sim 0.001$  pc ( $R_s = 2GM/c^2$  and  $M = 10^8 M_\odot$ ), and the gamma-ray emitting region  $R_\gamma \sim 0.1$  pc, the angle between the jet direction and the travelling direction of UV photons at  $R_\gamma$  is  $\sim \arcsin R_D/R_\gamma \sim 0.57^\circ$ . Then the photons within the radiation cone have the collision angles of  $\theta \lesssim 4.4^\circ$ . For the UV photons at the frequency  $\nu \simeq 10^{16.5}$  Hz with energies of  $\varepsilon_2 \simeq 2.56 \times 10^{-4}$  and these gamma-rays of  $\varepsilon_1 \simeq 3.91 \times 10^5$  corresponding to energies around 200 GeV, the left of equation (3) has a upper limit of  $\lesssim 0.15$ , which is less than the value at the right of equation (3), and then the two kinds of photons cannot be absorbed by the photon-photon pair creation processes. Therefore, the central UV radiation have negligible contributions to the absorption for gamma-rays relative to the diffuse radiation from the BLRs.

The energies carried by the annihilated gamma-rays would be deposited in the lower frequency radiation field by the synchrotron and inverse Compton processes of the electron-positron pairs and the pair cascade and pair annihilation processes (see Protheroe & Stanev 1993; Saugé & Henri 2004; Zdziarski & Coppi 1991). The intense creation of pairs would produce a strong radiation at low energy X-rays or at GeV energy (Protheroe & Stanev 1993; Saugé & Henri 2004; Zdziarski & Coppi 1991). The electron-positron pair cascade can cause the soft X-ray excesses (Zdziarski & Coppi 1991). The produced electron-positron pairs could make a difference at lower energies, around 1 GeV, where the pileup of photons below the absorption feature results in a significant flattening in the observed spectrum relative to the emission spectrum (Protheroe & Stanev 1993). Then the electron-positron pairs produced by the photon-photon annihilation processes in FSRQs could result in the similar observational effects mentioned above at around 1 GeV gamma-rays or low energy X-rays.

In summary, we used a BLR model to study the photon-photon absorption optical depth for gamma-rays with energies from 10 to 200 GeV in the observed spectrum. There are four key parameters for the BLR model: the gamma-ray emitting radius  $R_\gamma$ , the BLR luminosity  $L_{\text{BLR}}$ , the half thickness of BLR  $h$  and the ratio  $\tau_{\text{BLR}}/f_{\text{cov}}$ . The BLR luminosity  $L_{\text{BLR}}$  determines the distance  $r_{\text{BLR}}$ , which limits the BLR inner and outer radii of  $r_{\text{BLR,in}}$  and  $r_{\text{BLR,out}}$  if the parameter  $h$  is given. We discussed the dependence of the optical depth  $\tau_{\gamma\gamma}$  on the parameters  $R_\gamma$ ,  $h$  and  $r_{\text{BLR}}$ . The diffuse external radiation energy density in the gamma-ray emitting region is typically on the order of  $U_{\text{ph}} \sim 10^{-2}$  erg cm $^{-3}$  for FSRQs, and the ratio  $\tau_{\text{BLR}}/f_{\text{cov}}$  might be typically on the order of  $\tau_{\text{BLR}}/f_{\text{cov}} \sim 1$  for blazars. Then the inner and outer radii of BLR are required to be around  $r_{\text{BLR,in}} \sim 0.2$  pc and  $r_{\text{BLR,out}} \sim 0.6$  pc,

respectively. It is impossible for gamma-rays from 10 to 200 GeV emitted by FSRQs to escape from the diffuse radiation fields of the BLRs if  $R_\gamma \sim r_{\text{BLR,in}}$  (see Fig. 7). If *GLAST* could detect gamma-rays with energies from 10 to 200 GeV for most of FSRQs, there would be  $R_\gamma > r_{\text{BLR,in}}$  for FSRQs on average, otherwise,  $R_\gamma \lesssim r_{\text{BLR,in}}$ . If  $\tau_{\text{BLR}}/f_{\text{cov}} \sim 1/3$  and  $R_\gamma \sim r_{\text{BLR,in}}$  for the classical FSRQ 3C 279, the diffuse soft photon field is not transparent to gamma-rays with energies from multi-ten to 200 GeV and is transparent to gamma-rays around 10 GeV. *GLAST* observations in the energy domain of multi-ten to 200 GeV could limit constraints on the position of the gamma-ray emitting region relative to the inner radius of BLR and the BLR properties for 3C 279. For the powerful HFSRQ PKS 0405–123, the diffuse photon field is not transparent to gamma-rays with energies from 10 to 200 GeV in the observed spectrum. *GLAST* observations in the future could limit constraints on the gamma-ray emitting region and the BLR in this HFSRQ. Our results are model dependent, especially dependent on the gamma-ray emitting radius  $R_\gamma$  and the inner radius  $r_{\text{BLR,in}}$ . To determine the relationship of the inner radius  $r_{\text{BLR,in}}$  with the radius  $r_{\text{BLR}}$  derived from the reverberation mapping needs more theoretical and observational researches. *GLAST* observations in the future can give more observational constraints on the gamma-ray emitting regions and the BLRs for the powerful blazars.

We are grateful to the anonymous referee for his/her constructive comments and suggestions that helped to significantly improve this paper. This work is supported by National Natural Science Foundation of China (Grant 10443003, 10573030, and 10533050) and Natural Science Foundation of Yunnan Province (Grant 2003A0025Q). J.M.B. thanks support of the Bai Ren Ji Hua project of the CAS, China.

## REFERENCES

- Aharonian, F. et al., 2005, *A&A*, 437, 95  
 Albert, J. et al., 2006, *ApJ*, 637, L41  
 Baixeras, C. et al., 2004, *NIMPA*, 518, 188  
 Blandford, R. D., & Levison, A. 1995, *ApJ*, 441, 79  
 Blandford, R. D., & Rees, M. J. 1978, in *Pittsburgh Conf. on BL Lac Objects*, ed. A. M. Wolfe (Pittsburgh: Univ. Pittsburgh Press), 328  
 Böttcher, M. 1999, in *AIP Conf. Proc. 515, GeV-TeV Gamma Ray Astrophysics Workshop*, ed. B. L. Dingus, M. H. Salamon, & D. B. Kieda (New York: AIP), 31  
 Cao, X. W., & Jiang, D. R. 1999, *MNRAS*, 307, 802

- Catanese, M., et al. 1997, *ApJ*, 487, L143
- Chen, A., Reyes, L. C., & Ritz, S. 2004, *ApJ*, 608, 686
- Coppi, P. S. & Blandford, R. D. 1990, *MNRAS*, 245, 453
- D’Elia, V., Padovani, P., & Landt H. 2003, *MNRAS*, 339, 1081
- Donea, A. C., & Protheroe, R. J. 2003, *Astropart. Phys.*, 18, 377
- Fichtel, C. E., et al. 1994, *ApJS*, 94, 551
- Francis, P. J., Hewett, P. C., Foltz, C. B., Chaffee, F. H., Weymann, R. J., & Morris, S. L. 1991, *ApJ*, 373, 465
- Funk, S. et al., 2004, *Astropart. Phys.*, 22, 285
- Gaskell, C. M., Shields, G. A., & Wampler, E. J. 1981, *ApJ*, 249, 443
- Gehrels, N., & Michelson, P. 1999, *Astropart. Phys.*, 11, 277
- Georganopoulos, M. 2000, *ApJ*, 543, L15
- Georganopoulos, M., Kirk, J. G., & Mastichiadis, A. 2001, in *ASP Conf. Series 227, Blazar Demographics and Physics*, Ed. P. Padovani and C. M. Urry (San Francisco: Astronomical Society of the Pacific), 116
- Ghisellini, G., & Madau, P. 1996, *MNRAS*, 280, 67
- Ghisellini, G., Celotti, A., Fossati, G., Maraschi, L., & Comastri, A. 1998, *MNRAS*, 301, 451
- Gould, R. J. & Schroder, G. P. 1967, *Phys. Rev.*, 155, 1404
- Hartman, R. C., et al. 2001, *ApJ*, 553, 683
- Hinton, J. A. 2004, *New Astron. Rev.*, 48, 331
- Hofmann, W. 2003, *Proc. 28th ICRC (Tsukuba)*, 2811
- Jauch, J. M., & Rohrlich, F. 1976, *The theory of photons and electrons, The relativistic quantum field theory of charged particles with spin one-half (Texts and Monographs in Physics, New York: Springer, 1976, 2nd ed.)*
- Kaspi, S. & Netzer, H. 1999, *ApJ*, 524, 71
- Kaspi, S. 2000, in *ASP Conf. Proc. 224, Probing the Physics of Active Galactic Nuclei*, Ed. B. M. Peterson, R. W. Pogge, & R. S. Polidan (San Francisco: ASP), 347
- Lin, Y. C., et al. 1997, *ApJ*, 476, L11
- Lindfors, E. J., Valtaoja, E., & Turler, M. 2005, *A&A*, 440, 845
- Maiolino, R., Salvati, M., Marconi, A., & Antonucci, R. R. J. 2001, *A&A*, 375, 25

- Mukherjee, R., et al. 1997, *ApJ*, 490, 116
- Padovani, P., Costamante, L., Ghisellini, G., Giommi, P., & Perlman, E. 2002, *ApJ*, 581, 895
- Padovani, P., Perlman, E. S., Landt, H., Giommi, P., & Perri, M. 2003, *ApJ*, 588, 128
- Peterson, B. M. 1993, *PASP*, 105, 247
- Perlman, E. S., Padovani, P., Giommi, P., Sambruna, R., Jones, L. R., Tzioumis, A., & Reynolds, J. 1998, *AJ*, 115, 1253
- Protheroe, R. J., & Stanev, T. 1993, *MNRAS*, 264, 191
- Punch, M., et al. 1992, *Nature*, 358, 477
- Quinn, J., et al. 1996, *ApJ*, 456, L83
- Saugé, L., & Henri, G. 2004, *ApJ*, 616, 136
- Sokolov, A. & Marscher, A. P. 2005, *ApJ*, 629, 52
- Sulentic, J. W., Marziani, P., & Dultzin-Hacyan, D. 2000, *ARA&A*, 38, 521
- Thompson, D. J., et al. 1995, *ApJS*, 101, 259
- Thompson, D. J., et al. 1996, *ApJS*, 107, 227
- Urry, C. M. & Padovani, P. 1995, *PASP*, 107, 803
- Villata, M., et al. 1997, *A&AS*, 121, 119
- von Montigny, C., et al. 1995, *ApJ*, 440, 525
- Wehrle, A. E., et al. 1998, *ApJ*, 497, 178
- Wu, X. B., Wang, R., Kong, M. Z., Liu, F. K., & Han, J. L. 2004, *A&A*, 424, 793
- Zdziarski, A. A., & Coppi, P. S. 1991, *ApJ*, 376, 480

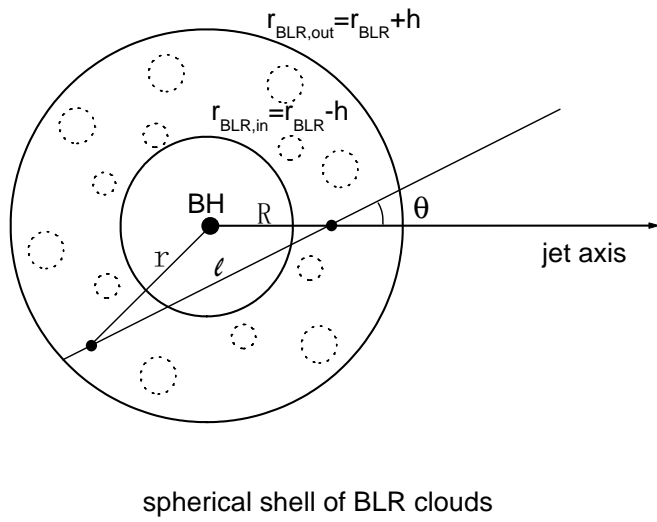


Fig. 1.— Sketch of axial cross section illustrating the geometry used for computation of the intensity of the BLR radiation and similar to Fig. 4 of Donea & Protheroe (2003).

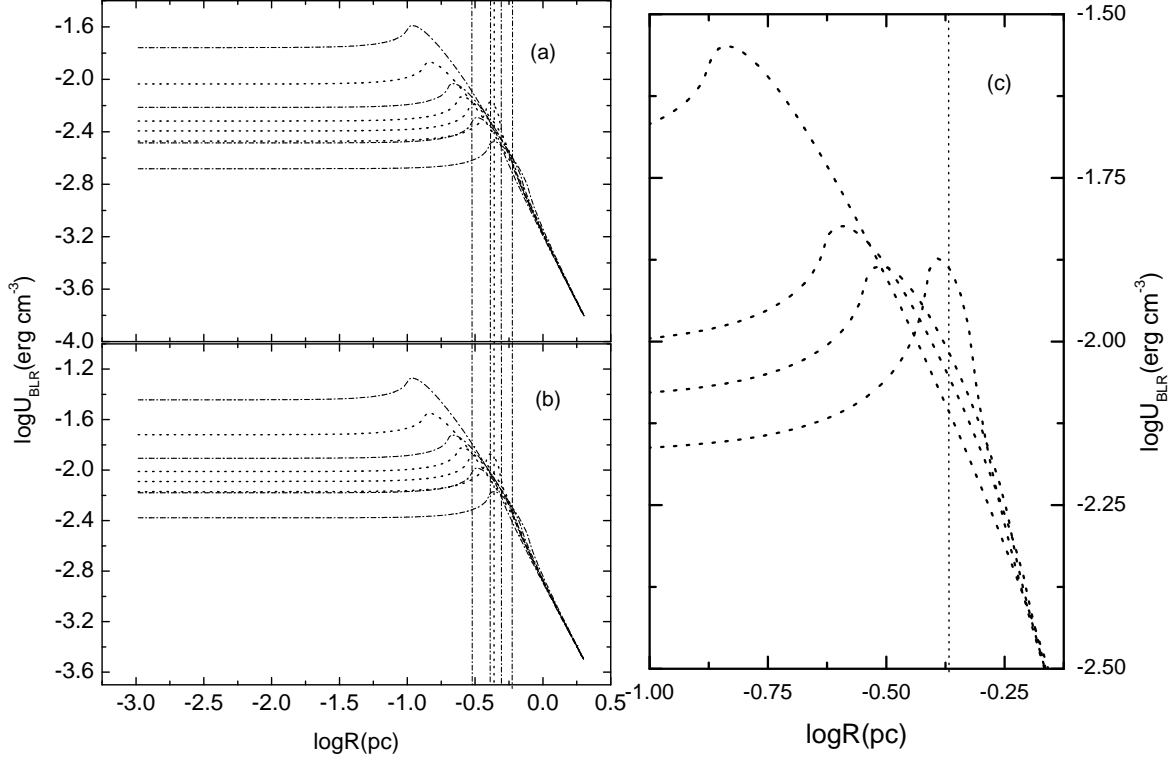


Fig. 2.— The radial dependence of the energy density on the parameters  $r_{\text{BLR}}$  and  $h$ . The dotted curves in plots are calculated by adopting  $L_{\text{BLR}} = 10^{45.35} \text{ erg s}^{-1}$ ,  $r_{\text{BLR}} = 0.43 \text{ pc}$ , and  $\tau_{\text{BLR}}/f_{\text{cov}} = 1$ . From the bottom up, the four dotted curves have the parameter  $h$  at 0.05, 0.15, 0.20, and 0.30 pc. The dash-dotted curves are calculated by adopting  $L_{\text{BLR}} = 10^{45.35} \text{ erg s}^{-1}$ ,  $h = 0.20 \text{ pc}$ , and  $\tau_{\text{BLR}}/f_{\text{cov}} = 1$ . From the top down, the four dash-dotted curves have the parameter  $r_{\text{BLR}}$  at 0.30, 0.40, 0.50, and 0.60 pc. The plot (a) presents the energy density distributions for the emission lines, and the plot (b) presents the corresponding energy density distributions for the emission lines and continuum radiation. The plot (c) is the zoomed parts for the four dotted curves in the plot (b). The dotted vertical lines correspond to  $r_{\text{BLR}} = 0.43 \text{ pc}$ , and the dash-dotted vertical lines correspond to  $r_{\text{BLR}}$  at 0.30, 0.40, 0.50, and 0.60 pc.

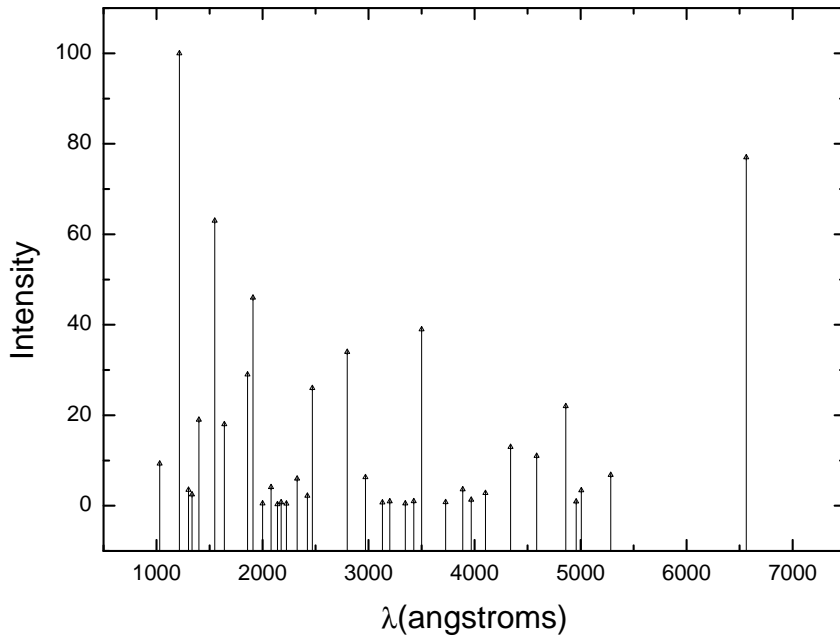


Fig. 3.— The relative intensity of broad emission lines adopted by us.

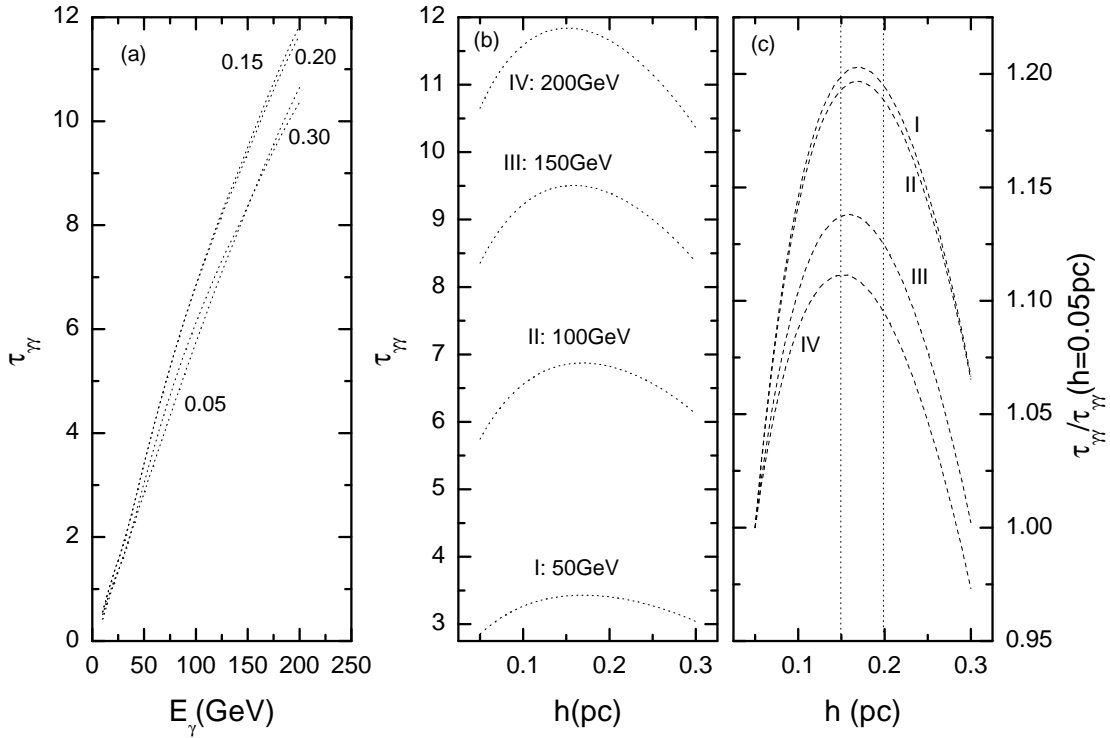


Fig. 4.— The dependence of  $\tau_{\gamma\gamma}$  on the parameter  $h$ . In the calculations, we used  $r_{\text{BLR}} = 0.43$  pc and assumed  $R_\gamma = r_{\text{BLR}}$  and  $\tau_{\text{BLR}}/f_{\text{cov}} = 1$ . The plot (a) is the photon-photon optical depth for four values of  $h$ , and the numbers attached to the four curves give  $h$  in pc. The plot (b) is the dependence of  $\tau_{\gamma\gamma}$  on  $h$  for four values of  $E_\gamma$ . The plot (c) is the normalized  $\tau_{\gamma\gamma}$  corresponding to the four cases in the plot (b).

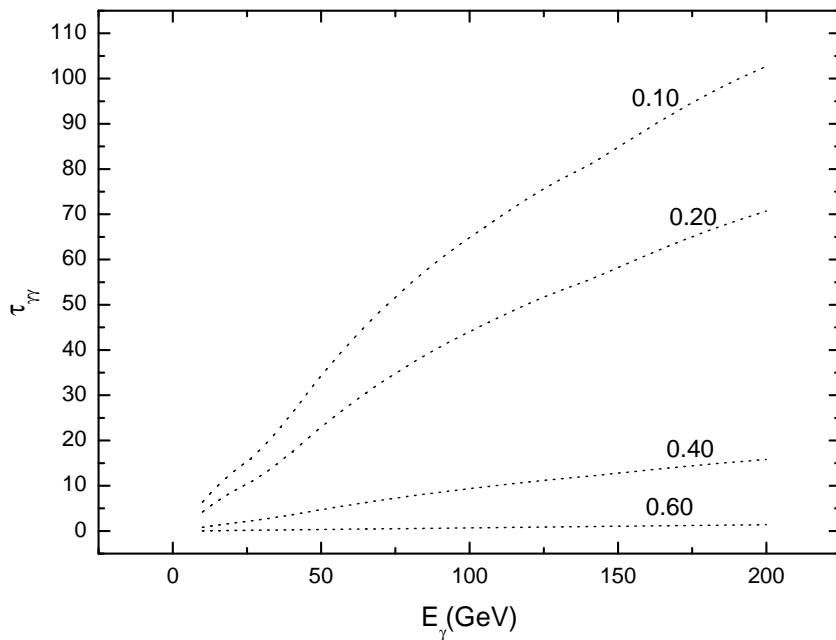


Fig. 5.— The dependence of  $\tau_{\gamma\gamma}$  on the parameter  $R_\gamma$ , and numbers attached to the curves give  $R_\gamma$  in pc. In the calculations,  $r_{\text{BLR}} = 0.43$  pc,  $h = 0.20$  pc and  $\tau_{\text{BLR}}/f_{\text{cov}} = 1$  are assumed.

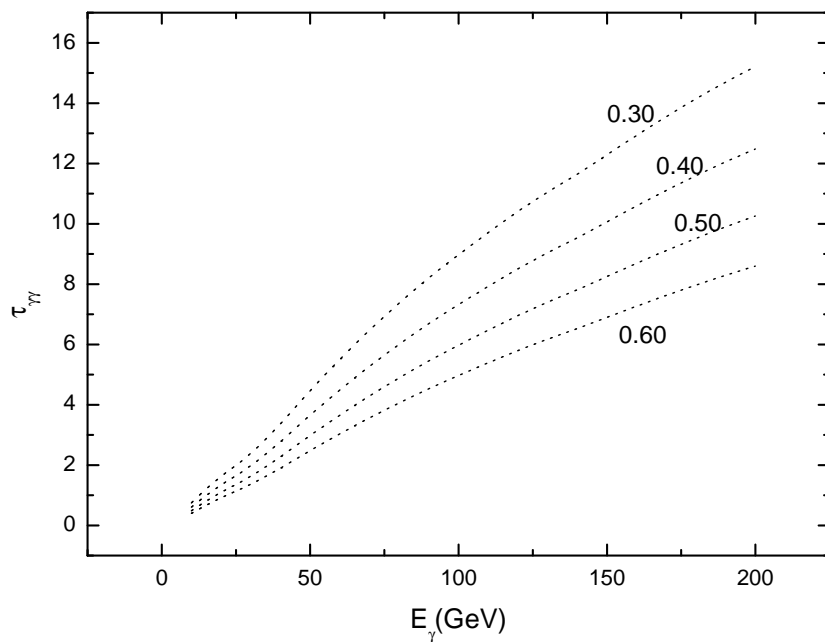


Fig. 6.— The dependence of  $\tau_{\gamma\gamma}$  on the parameter  $r_{\text{BLR}}$ , and numbers attached to the curves give  $r_{\text{BLR}}$  in pc. In the calculations,  $R_\gamma = r_{\text{BLR}}$ ,  $h = 0.20$  pc, and  $\tau_{\text{BLR}}/f_{\text{cov}} = 1$  are assumed.

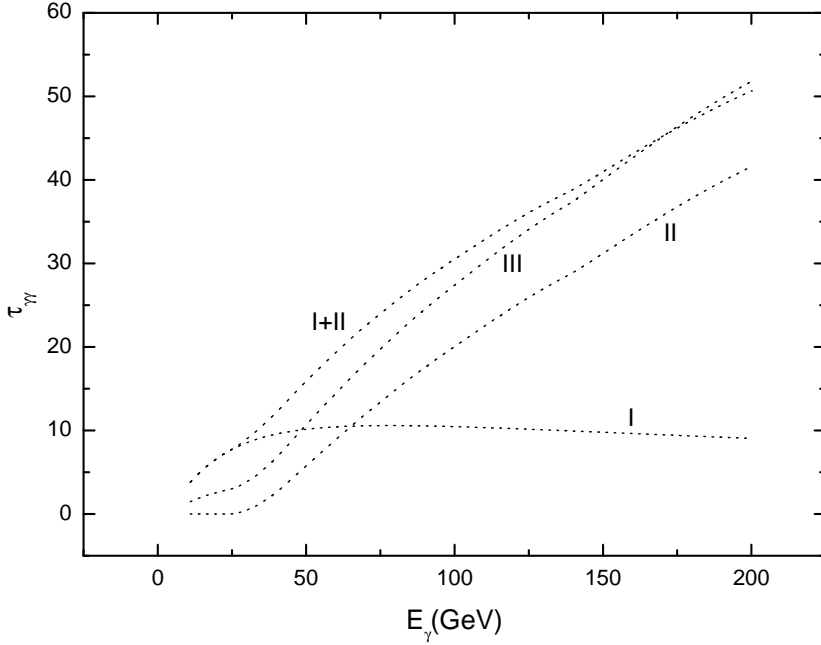


Fig. 7.— The optical depth of photon-photon absorption for FSRQs. The curve I corresponds to the absorption by the diluted blackbody radiation, the curve II the absorption by the emission lines, and the curve I+II the sum of the curves I and II. The three curves are calculated by adopting  $r_{\text{BLR}} = 0.43$  pc,  $h = 0.20$  pc,  $R_\gamma = r_{\text{BLR},\text{in}}$ , and  $\tau_{\text{BLR}}/f_{\text{cov}} = 1$ . The curve III corresponds to the optical depth by adopting  $r_{\text{BLR},\text{in}} = 0.2$  pc,  $r_{\text{BLR},\text{out}} = 0.6$  pc,  $\tau_{\text{BLR}}/f_{\text{cov}} = 1/3$ , and  $R_\gamma = r_{\text{BLR},\text{in}}$ .

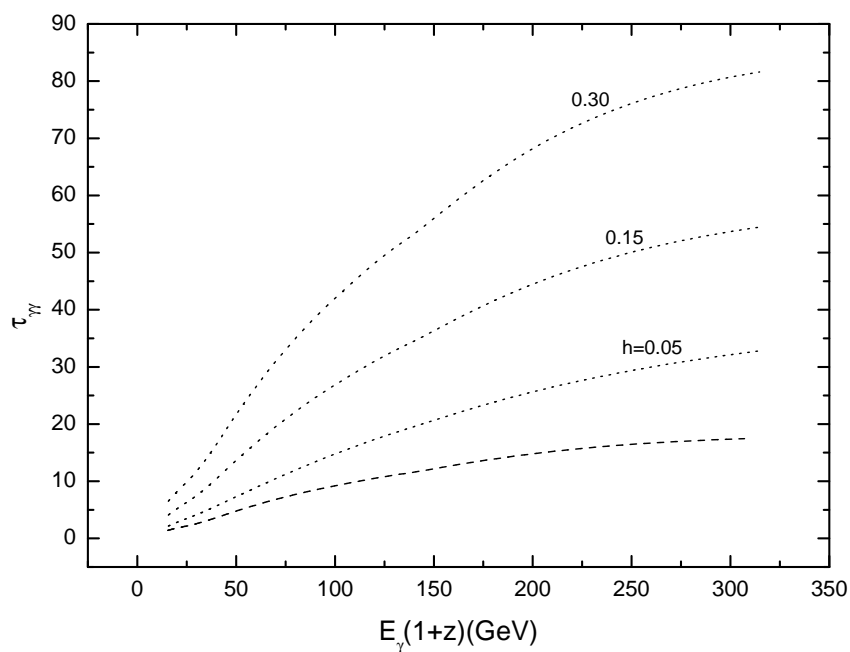


Fig. 8.— The photon-photon optical depth for HFSRQ PKS 0405–123 are presented by the dotted curves, and numbers attached to the curves give  $h$  in pc. The dashed curve is the photon-photon optical depth for 3C 279, adopting  $r_{\text{BLR},\text{in}} = 0.1$  pc and  $r_{\text{BLR},\text{out}} = 0.4$  pc. In the calculations,  $R_\gamma = r_{\text{BLR},\text{in}}$  and  $\tau_{\text{BLR}}/f_{\text{cov}} = 1$  are assumed.